

Joint Effects of Radio Channels and Node Mobility on Link Dynamics in Wireless Networks

Wenye Wang Ming Zhao

Department of Electrical and Computer Engineering
North Carolina State University, Raleigh, NC 27695

Abstract—In this paper, we study link properties over dynamic radio channels based on analytical models and simulations. Specifically, channel variability and mobility are investigated through two quantities: *effective transmission range* and *node-pair distance*, respectively. We find that the PDF of link lifetime can be approximated by exponential distribution with parameter characterized by the ratio of average node speed to effective transmission range. Moreover, we show that average link lifetime for slower mobile nodes is mainly determined by radio channel characteristics, whereas for faster mobile nodes, it is dominated by node mobility. Through analysis and simulations, we find that the impacting factors on residual link lifetime are in the decreasing order of average node speed, effective transmission range, and node-pair distance on the fly. We further present the implication and application of link properties to path lifetime, network connectivity, and routing performance.

I. INTRODUCTION

Link and path properties are essential to applications and performance in mobile ad hoc networks (MANETs) because they have direct impact on many performance metrics, such as connection time, end-to-end delay, packet losses, and throughput. In turn, they are closely dependent on time-varying radio environment and node mobility. There has been a large number of studies examining the effect of node mobility on link dynamics, such as link lifetime [1]–[5], link change rate [3], [6], link residual time and link availability [3], [5], [7], [8]. The main results in previous studies include: i) There exists a peak in the link lifetime distribution based on random mobility models [1]–[3]. ii) For a k -hop path, when $k \rightarrow \infty$, the path lifetime distribution converges to exponential distribution with the parameter of the sum of the inverses of the expected link durations [9], whereas $k \geq 4$ for simulation results [2]. iii) The PDF of link change inter-arrival time can be approximated by an exponential distribution with fairly high accuracy [3], and iv) Markovian model is an effective method to study relative movements and distance of a node-pair [4], [5].

The limitations of existing works on link dynamics are three-fold. First, existing random mobility models, such as random waypoint model (RWP) and its variants, have significant drawbacks toward the steady-state properties of moving speed and nodal distribution, which could lead to defective analysis and simulations on link studies [10]. Second, the time-scale of random mobility models (e.g., moving duration) is generally much larger than the time-scale of dynamic radio channels

which may change rapidly and distinctly over short distance and time [11], [12]. However, the study in [13] suggested instead the time scale used to describe node mobility should be less than the time scale for capturing the significant channel variability. Third, it is assumed in previous studies that transmission range of each node is constant regardless of moving scenarios. This is helpful in simplifying the analysis, at the cost of ignoring the effect of radio environments. For instance, Bettstetter provided a wireless channel model and studied how shadow fading affects the topology and connectivity of wireless multi-hop networks [14]. Correspondingly, Yang et al. in [15] proposed a link-stability prediction method based on timely user movement information and received signal strength in shadowed environments. In [13], the authors showed that the relative movement of the transmitter-receiver pair can cause significant channel variability, due to the time-varying multipath propagation, mobility and multiuser interference. Therefore, considering both node mobility and radio environments at similar time-scale is critical to better understanding link and path properties in MANETs.

Although existing literatures provide constructive solutions on link dynamics of MANETs, it still remains elusive for understanding the impacts of these two independent, yet simultaneously forcible factors (radio channels and smooth node mobility) on link dynamics with respect to various network scenarios. The answers to the question will provide essential guidelines on all related issues such as designing routing protocols [2], [3], [16], improving network performance [13], [17] and optimizing topology control [12], [14].

As the optimal and fixed radio transmission range are rarely achieved in real dynamic wireless channels, in this paper, we introduce an *effective transmission range* (ETR) by using radio fading models [12], which are simple, and closely capture *large-scale* propagation, i.e., *path loss*, *shadowing effect*, and *multi-path fading* of wireless links [11]. Hence, the link lifetime between a pair of nodes is determined concurrently by ETR and timely node-pair distance upon smooth node mobility [10]. Somewhat surprisingly, we show that link lifetime distribution can be effectively approximated by an exponential distribution, which is in contrast with previous studies that there exists a peak in the distribution function which are mainly obtained from random mobility models [1]–[3]. More interestingly, the exponential distribution parameter can be simplified by $\frac{\bar{V}}{R_e}$, where \bar{V} is the average speed and R_e is the ETR of a mobile node. Since the path lifetime is

This work is supported in part by the National Science Foundation under award CNS-0546289.

determined by the minimum link lifetime en route, we can easily conclude that the PDF of path lifetime also follows exponential distribution, which greatly relaxes the assumption of large (approach to infinite) hop-count of a path for its distribution converging to exponential [9]. We also find that the impacting factors on both link and residual link lifetime are in the decreasing order of average node speed, ETR, and node-pair distance.

Although the main objective of this work is to provide fundamental understanding on link lifetime distribution in Section III, and average link lifetime in Sections IV, our results do have direct implications to network connectivity and performance as shown in Section V.

II. CHARACTERIZATION OF RADIO LINKS AND MOBILITY

A. Effective Transmission Range

In mobile radio environments, the received signal is generally influenced by three fading effects: large-scale path loss, multi-path fading, and shadowing [11]. For instance, in vehicular movements, mobile nodes usually move at high speeds, so that the *large-scale path loss*, can be the dominant factor affecting the signal strength with increasing distance. On the other hand, the relative movement of two persons inside a building may be over a short travel distance (order of wavelengths), which is mainly constrained by *small-scale fading*, also called multi-path fading. Due to the presence of obstacles in the propagation channel, the signal also undergoes *shadowing* loss. Fig. 1 shows an example of the probability of link connection between two nodes under different fading conditions upon transmission distance. When the transmission distance is 200 m, it is observed that the probability of link connection is decreased from 1 (with the large-scale path loss only) to 0.5 when shadow fading is considered, and it further reduces to 0.28 if all these three propagation mechanisms are in effect. Clearly, the valid node transmission range becomes a random variable featured by channel fading parameters.

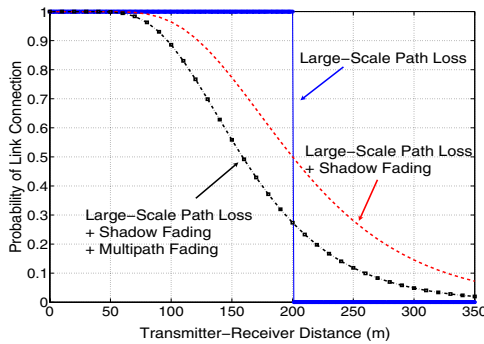


Fig. 1. Probability of link connection between two nodes, where path loss exponent $\xi = 3$, shadow fading $\sigma_s = 5$ dB, and multi-path fading is 3 dB.

In [18], it is showed that in general the link and connectivity analysis given the geometric disc abstraction holds for more irregular shapes of a node transmission zone. Therefore, we introduce a novel metric: *Effective Transmission Range* (ETR) to capture the effect of radio propagation mechanisms.

Definition 1: In a radio channel characterized by the path loss exponent ξ , shadowing X_{σ_s} and multi-path fading χ^2 , *Effective Transmission Range* (ETR), denoted by R_e , is the maximum value of the transmission range R , which holds the condition $P_{r,dB} \geq P_{0,dB}$ with a very high probability (w.h.p.) $\mathbb{P} = 99\%$, where $P_{r,dB}$ is the received signal power and $P_{0,dB}$ is the threshold of the receiving power.

Let $\tilde{P}_{dB} = P_{t,dB} - \bar{L}_{0,dB} - 10 \log_{10} E\{\chi^2\}$, where $P_{t,dB}$ is the transmission power, and $\bar{L}_{0,dB}$ is the average path loss at the reference point that is 1 meter away from the transmitter. $10 \log_{10} E\{\chi^2\}$ is the average multi-path fading in dB [11]. The probability \mathbb{P} , i.e. $Pr\{P_{r,dB} \geq P_{0,dB}\}$ is represented as:

$$\begin{aligned} \mathbb{P} &= Pr\{\tilde{P}_{dB} - 10\xi \log_{10} R_e - X_{\sigma_s} \geq P_{0,dB}\} \\ &= \frac{1}{\sqrt{2\pi}\sigma_s} \int_{-\infty}^{\tilde{P}_{dB} - 10\xi \log_{10} R_e - P_{0,dB}} \exp\left(-\frac{x^2}{2\sigma_s^2}\right) dx \\ &= \frac{1}{2} \left[1 - \operatorname{erf}\left(\frac{10\xi \log_{10} R_e + P_{0,dB} - \tilde{P}_{dB}}{\sqrt{2}\sigma_s}\right)\right], \end{aligned} \quad (1)$$

where $\operatorname{erf}(\cdot)$ is the error function, defined by $\operatorname{erf}(z) = \int_0^z \frac{2}{\sqrt{\pi}} e^{-x^2} dx$. From the Definition 1, we have

$$\begin{cases} \frac{1}{2} \left[1 - \operatorname{erf}\left(\frac{10\xi \log_{10} R_e + P_{0,dB} - \tilde{P}_{dB}}{\sqrt{2}\sigma_s}\right)\right] = \mathbb{P} = 0.99, \\ \frac{10\xi \log_{10} R_e + P_{0,dB} - \tilde{P}_{dB}}{\sqrt{2}\sigma_s} = -1.65. \end{cases} \quad (2)$$

Hence, upon (2), we obtain the ETR, denoted by R_e , of mobile nodes with specific requirements in a radio environment:

$$\log_{10} R_e = \frac{-2.33\sigma_s + \tilde{P}_{dB} - P_{0,dB}}{10\xi}. \quad (3)$$

If we assume that same type of mobile nodes uses same transmission power and receiving power threshold, then $P_{t,dB} - \bar{L}_{0,dB} - P_{0,dB}$ is a constant value denoted by c . From (3), we find that R_e is a function of three fading parameters:

$$R_e = f(\xi, \sigma_s, \chi) = 10^{\frac{-2.33\sigma_s - 10 \log_{10} E\{\chi^2\} + c}{10\xi}}. \quad (4)$$

As an illustration, from (4), we find that an increase of 1 dB in either σ_s or $E\{\chi^2\}$ only, R_e will be decreased by 16% and 7%, respectively. While when path loss exponent ξ increases by 1, e.g. from 3 to 4, R_e will decrease around 30%.

Remark 1: The impacting weight of channel fading on ETR is in the decreasing order of path loss (ξ), shadow fading (X_{σ_s}), and multi-path fading (χ^2).

B. Smooth Node Mobility

It is worth noting that the time-scale of wireless channels is closely dependent on radio propagations. In particular, the path loss is the function of distance, and does not vary with time. As the shadow fading varies with travel distance on the order of tens or hundreds of meters, it generally would not vary within a short time interval. In contrast, the multi-path fading changes within small distance and the fading changing rate is proportional to the receiver velocity. Hence, multi-path fading changes in the order of seconds [11]. Therefore, in order to observe the concurrent influence of radio channels and

mobility on link lifetime, we must consider the characteristics of node mobility in the similar time-scale of radio channels.

Therefore, in this paper, we use the smooth mobility model in [10] in that this model allows flexible, small equal-length time steps (Δt) for smooth movement description. The model complies with the physical law of smooth motion: each node evenly accelerates its speed to the target speed of the movement initially, and evenly decelerates speed before a full stop. Furthermore, the model has nice steady-state properties of uniform nodal distribution and stable moving speed.

C. Node-Pair Distance

The distance between two mobile nodes is denoted by *Node-Pair Distance*, ρ , which is dependent on the relative movements of two nodes. For instance, ρ_m represents the distance between two nodes after m time steps [10]. As an example, Fig. 2(a) illustrates the relationship between the maximum transmission range R_{\max} and node-pair distance ρ_m under different radio environments. Thus, by comparing the value between the time-varying variable R_{\max} and ρ_m at each time step (normalized to 1 second per time step Δt), the corresponding link existence can be obtained, which is shown in Fig. 2(b). It is evident that the link lifetime and breakage rate can vary dramatically under different radio channels. For instance, the frequency of link breakage under channels with additional shadowing and multi-path fading is about 19 times higher than that with path loss only, which is the inverse of average link lifetime.

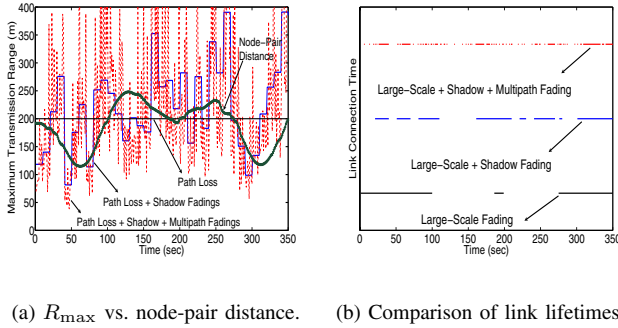


Fig. 2. Illustration of maximum transmission range R_{\max} vs. link lifetime under different radio channel fading, for average node speed of 2 m/sec.

As shown in Fig. 2(a), given a specific radio environment, the maximum transmission range R_{\max} between two nodes varies dramatically with time. Accordingly, the effective transmission range R_e , defined in (3), can efficiently characterize the valid transmission distance with specific radio fading. In fact, the similar concept of ETR has been already applied in the real industrial world. For example, the Accutech wireless instrumentation products use 1/3 of the maximum transmission range R_{\max} as the rule-of-thumb for working transmission range [19]. Therefore, the above observations motivate us to analyze the probability distribution of link lifetime by comparing effective transmission range R_e with node pair distance ρ_m .

Remark 2: For a pair of nodes (u, w) , there exists a link between them if and only if their distance ρ_m is no greater than their symmetric effective transmission range R_e .

Thus, the link lifetime T_L , in essence, is defined as

$$T_L \triangleq \sup_{m>0} \{m \cdot \Delta t : \max \rho_m \leq R_e\}. \quad (5)$$

Note that the node-pair distance ρ_m is dependent on node mobility. Hence, in the next section, we start with the relative movement of a node-pair upon smooth mobility model, and then we derive the link lifetime distribution.

III. LINK LIFETIME DISTRIBUTION

A. Relative Movement: Speed and Distance

For a node-pair (u, w) , we use node u as the reference node, which lies in the center of its transmission zone with radius of the effective transmission range R_e . As explained in previous section, we use the smooth mobility model [10] in order to match the time-scale variation of radio channels [13] and smooth motion of moving nodes. Thus, the relative distance of a node-pair can be represented by relative positions at each time step. An example of the relative movement trajectory is illustrated in Fig. 3. We denote v_m as the magnitude of the relative speed vector \vec{v}_m . After the m^{th} time step relative movement, node w lies at the position represented by (X_m, Y_m) . Correspondingly, ρ_m , the node-pair distance, is the magnitude of the vector $\vec{\rho}_m$, such that $\rho_m = \sqrt{X_m^2 + Y_m^2}$. We assume that the relative speed v_m and the angle ψ_m of node w are i.i.d. RVs, then the coordinate X_m and Y_m can be approximated by Gaussian random distribution, when $m \gg 1$ [7]. For simplicity, we normalize Δt to 1 second throughout, then the m^{th} step relative speed v_m is:

$$v_m = |\vec{v}_m| = \sqrt{(X_m - X_{m-1})^2 + (Y_m - Y_{m-1})^2}, \quad (6)$$

where both RV $(X_m - X_{m-1})$ and $(Y_m - Y_{m-1})$ can be effectively approximated by an identical Gaussian distribution with zero mean. Thus, upon the same arguments in [7], when $m \gg 1$, v_m can be further effectively approximated by a *Rayleigh density* represented as:

$$f_Z(z) = \frac{z}{\alpha^2} e^{-\frac{z^2}{2\alpha^2}} U(z) \quad \text{and} \quad E\{z\} = \alpha\sqrt{\pi/2}, \quad (7)$$

where α is the parameter of the Rayleigh distribution [20]. To simplify the analysis, we assume that mobile nodes have the same average moving speed \bar{V} , though with different mobility pattern. Then the range of relative speed of two nodes is over $[0, 2(\bar{V} + \delta_V)]$, depending on either two node moving along the same direction or the opposite direction, where δ_V is the maximum speed deviation of \bar{V} in one movement introduced in the smooth model [10]. Corresponding to (7), $\bar{V} = \alpha\sqrt{\pi/2}$, then the PDF of relative speed is:

$$f_V(v) = \frac{v}{(\bar{V}\sqrt{\frac{2}{\pi}})^2} e^{-\frac{v^2}{2(\bar{V}\sqrt{\frac{2}{\pi}})^2}} = \frac{\pi v}{2\bar{V}^2} e^{-\frac{\pi v^2}{4\bar{V}^2}}. \quad (8)$$

To validate the expression in (8), we obtain the relative speed distribution $f_V(v)$ between two nodes by simulations

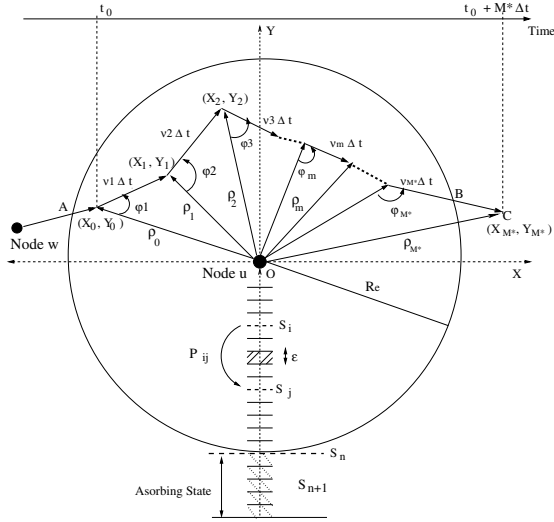


Fig. 3. Relative movement trajectory of node-pair (u, w) .

under different levels of node speed. Fig. 4 illustrates the PDF of relative speed resulted from both simulation and the theoretical expression from (8) versus different values of \bar{V} as [2, 5, 10, 15, 20] m/sec, respectively. It can be observed that the approximated Rayleigh distribution matches very well with the distribution of relative speed obtained by simulations.

Remark 3: The relative speed of a node-pair can be approximated by Rayleigh distribution not only for large-scale mobility [7], but also for small-scale smooth mobility. In fact, the smaller the time step of mobility modeling, the more accurate the approximation yields.

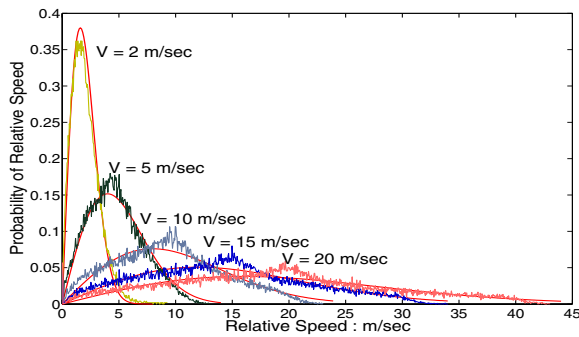


Fig. 4. Rayleigh distribution approximation of the relative speed.

As illustrated in Fig. 3, ρ_m is a random variable that depends on the current and next positions of node w in relation to node u . Specifically, at the m^{th} step, $\vec{\rho}_m = \vec{\rho}_{m-1} + \vec{v}_m$. Hence, ρ_m can be represented as:

$$\rho_m = |\vec{\rho}_m| = \sqrt{\rho_{m-1}^2 + v_m^2 - 2\rho_{m-1}v_m \cos \psi_m}, \quad (9)$$

where ψ_m is uniformly distributed from $[0, \pi)$. From (9), ψ_m can be represented as:

$$\psi_m = \arccos \frac{\rho_{m-1}^2 + v_m^2 - \rho_m^2}{2\rho_{m-1}v_m}. \quad (10)$$

We denote $f_{\rho_m|\rho_{m-1}}(\rho_m | \rho_{m-1})$ as the conditional distribu-

tion of relative distance, which is given by

$$\begin{aligned} & f_{\rho_m|\rho_{m-1}}(\rho_m | \rho_{m-1}) \\ &= \int_0^{2(\bar{V} + \delta_V)} f_{\rho_m|\rho_{m-1}, v_m}(\rho_m | \rho_{m-1}, v_m) \cdot f_V(v_m) dv_m \\ &= \int_0^{2(\bar{V} + \delta_V)} \frac{\frac{2}{\pi} \rho_m \cdot f_V(v_m) dv_m}{[4\rho_{m-1}^2 v_m^2 - (\rho_{m-1}^2 + v_m^2 - \rho_m^2)^2]^{1/2}}, \end{aligned} \quad (11)$$

where $f_V(v)$ is the PDF of the relative speed. Thus, the conditional probability of node-pair distance can be determined by substituting $f_V(v)$ obtained from (8) into (11). The result of (11) is useful in understanding the transition between two consecutive steps. However, it is not sufficient to know the node-pair distance at an arbitrary time instant, which is a time-varying variable. In order to examine the node-pair distance at each time step, the effective transmission range R_e of node u is quantized into n equal-length intervals with a width of ε meters. Hence, $R_e = n \cdot \varepsilon$, which indicates that there are n states within the transmission zone. Each interval ε is associated with a state representing the $u-w$ distance. For example, state S_i indicates that the $u-w$ distance interval is over the range $[(i-1)\varepsilon, i\varepsilon]$, which is shown in the lower half in Fig. 3. Note, since ε is a unit of distance interval, the number of states n is a variable in proportion to R_e , which is in turn characterized by the wireless environment.

B. Distance Transition Matrix \mathbf{P}

We denote \mathbf{P} as the distance transition probability matrix, to model the distance transition at each time step. Each element P_{ij} indicates the transition probability that $u-w$ distance is changed from current state S_i to next state S_j after one time step. From Fig. 3, the link expires after the M^{th} time step when the event of $\{\rho_{M^*} > R_e\}$ first happens. In addition, we use state S_{n+1} to represent all the $u-w$ distances that are greater than R_e . Since link connection breaks when node w reaches state S_{n+1} , we define state S_{n+1} as the *absorbing state* of matrix \mathbf{P} . This implies that \mathbf{P} is an n by $n+1$ matrix. The value of P_{ij} of matrix \mathbf{P} is essential to the analytical study of link dynamics. The details of how to find the link lifetime distribution by using \mathbf{P} will be explained in Section III-C. Next, we derive the approximation of P_{ij} based on node-pair distance distribution in (11).

First, the transition probability P_{ij} can be represented by:

$$\begin{aligned} P_{ij} &= \text{Prob}\{\rho_m \in S_j | \rho_{m-1} \in S_i\} \\ &= \frac{\text{Prob}\{(j-1)\varepsilon \leq \rho_m \leq j\varepsilon \cap (i-1)\varepsilon \leq \rho_{m-1} \leq i\varepsilon\}}{\text{Prob}\{(i-1)\varepsilon \leq \rho_{m-1} \leq i\varepsilon\}} \\ &= \frac{\int_{(j-1)\varepsilon}^{j\varepsilon} \int_{(i-1)\varepsilon}^{i\varepsilon} f_{\rho_m|\rho_{m-1}}(\rho_m | \rho_{m-1}) f(\rho_{m-1}) d\rho_{m-1} d\rho_m}{\int_{(i-1)\varepsilon}^{i\varepsilon} f(\rho_{m-1}) d\rho_{m-1}}. \end{aligned} \quad (12)$$

It is clear that (12) can be obtained by substituting (11) into it. However, we find the result of such an expression of (12) cannot be simplified to a closed-form representation and is too complicated for computation. Thus, we aim to derive an approximation of P_{ij} for easy analysis.

Theorem 1: The transition probability P_{ij} of matrix \mathbf{P} can be approximated by

$$\begin{cases} \tilde{P}_{ij} \approx \frac{0.2\varepsilon}{\bar{V}} \sqrt{\frac{2j-1}{2i-1}} \left[\ln \frac{4(\bar{V}+\delta_V)^2 - \varepsilon^2(j-i)^2(i+j-1)^2}{\varepsilon^2(i+j-1)^2 - 4(\bar{V}+\delta_V)^2(j-i)^2} \right]^{\frac{1}{2}} \\ P_{ij} = \tilde{P}_{ij} / \sum_j \tilde{P}_{ij} \quad \forall i. \end{cases} \quad (13)$$

Recall that \bar{V} represents average node speed and δ_V is the maximum variation of \bar{V} according to smooth model [10].

Proof: Let $f(x) = e^{\frac{-\pi x}{2\bar{V}}}$ and

$$g(x) = \left[4\rho_{m-1}^2 \rho_m^2 - [x - (\rho_{m-1}^2 + \rho_m^2)]^2 \right]^{-1/2}.$$

With (11), we can see that $f(x) > 0$ and $g(x) > 0$, when $x \in [0, 4(\bar{V} + \delta_V)^2]$. By using *Schwarz inequality* [20],

$$\int_a^b |f(x) \cdot g(x)| dx \leq \left[\int_a^b |f(x)|^2 dx \right]^{\frac{1}{2}} \left[\int_a^b |g(x)|^2 dx \right]^{\frac{1}{2}}. \quad (14)$$

we have

$$f_{\rho_m|\rho_{m-1}}(\rho_m | \rho_{m-1}) \leq \frac{\rho_m}{2\bar{V}^2} \left[\int_0^{4(\bar{V}+\delta_V)^2} e^{\frac{-\pi x}{2\bar{V}}} dx \right]^{\frac{1}{2}} \times \left[\int_0^{4(\bar{V}+\delta_V)^2} \frac{dx}{4\rho_{m-1}^2 \rho_m^2 - [x - (\rho_{m-1}^2 + \rho_m^2)]^2} \right]^{\frac{1}{2}}. \quad (15)$$

Then by respectively deriving the integral of $f(x)$ and $g(x)$, plus a bit work on simplification, the approximation of the conditional distribution $f_{\rho_m|\rho_{m-1}}(\rho_m | \rho_{m-1})$ can be:

$$f_{\rho_m|\rho_{m-1}}(\rho_m | \rho_{m-1}) \leq \frac{0.2}{\bar{V}} \sqrt{\frac{\rho_m}{\rho_{m-1}}} \times \left[\ln \frac{4(\bar{V} + \delta_V)^2 - (\rho_m - \rho_{m-1})^2(\rho_{m-1} + \rho_m)^2}{|(\rho_{m-1} + \rho_m)^2 - 4(\bar{V} + \delta_V)^2(\rho_m - \rho_{m-1})^2|} \right]^{\frac{1}{2}} \quad (16)$$

We further apply the Mean-Value theorem to derive the numerical solution of P_{ij} . In particular, according to P_{ij} defined in (12), where $(j-1)\varepsilon \leq \rho_m \leq j\varepsilon$ and $(i-1)\varepsilon \leq \rho_{m-1} \leq i\varepsilon$, if ε is sufficiently small, we can effectively use the middle point $i - \frac{\varepsilon}{2}$ and $j - \frac{\varepsilon}{2}$ to respectively represent the value of ρ_{m-1} and ρ_m [5]. For instance, $\int_{(i-1)\varepsilon}^{i\varepsilon} f(\rho_{m-1}) d\rho_{m-1} \approx \varepsilon \cdot f(i\varepsilon - \frac{\varepsilon}{2})$. With this argument and the result from (16), P_{ij} derived in (12) can be effectively approximated by \tilde{P}_{ij} :

$$\tilde{P}_{ij} \approx \varepsilon \cdot f_{\rho_m|\rho_{m-1}} \left[\left(j - \frac{1}{2} \right) \cdot \varepsilon \mid \left(i - \frac{1}{2} \right) \cdot \varepsilon \right] \quad (17)$$

By using the results from (16) and (17), we can obtain \tilde{P}_{ij} as shown in Theorem 1. Note, the approximation value of \tilde{P}_{ij} is normalized along each row of the matrix \mathbf{P} to guarantee the fundamental property of the transition matrix \mathbf{P} , i.e., $\sum_j P_{ij} = 1$, $\forall i, 1 \leq i \leq n$, as shown in (13). ■

To validate the accuracy of this approximate expression, we illustrate the computational error versus ε between the numerical result of P_{ij} from (12) and (13) in Fig. 5. Specifically, we set $\bar{V} = 15$ m/s, $R_e = 250$ m, the current state $i = 50$, and let ε vary from 1 m to 3 m. It is observed that, as ε decreases, the computational error is reduced, which is up to 0.02 when $\varepsilon = 1$ m. Therefore, we conclude that P_{ij} approximation can achieve fairly high accuracy when ε is sufficient small.

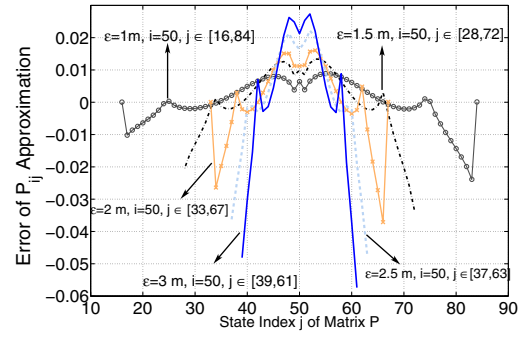


Fig. 5. Approximation of P_{ij} with respect to ε .

C. Approximation of Link Lifetime Distribution

Upon Fig. 3, a communication link between a node-pair forms immediately after the node w crosses the border of node u 's transmission zone at time t_0 . Recall that T_L denotes the link lifetime, which is the time node w continuously lies inside node u 's transmission zone. The link expires after the M^{th} time step when the node-pair distance is larger than ETR for the first time since t_0 . In this example, $T_L = M \cdot \Delta t$, hence T_L is a random variable from (5) and the CDF of link lifetime is $Prob\{T_L \leq m\}$ for $\Delta t = 1$ s.

Here, we derive the link lifetime distribution based on the distance transition matrix \mathbf{P} obtained in previous subsection. We denote by $\pi_i^{(m)}$ the probability that node w lies in state S_i after the m^{th} step, and $\pi^{(m)}$ is the row vector whose i^{th} element is $\pi_i^{(m)}$. That is $\pi^{(m)} = (\pi_1^{(m)}, \dots, \pi_i^{(m)}, \dots, \pi_{n+1}^{(m)})$. And $\pi^{(0)}$ denotes the probability of the initial state that node w lies when the link is initially formed, for instance, according to illustration in Fig. 3, at time t_0 , $\pi_i^{(0)} = Prob\{\rho_0 \in S_i\}$. For simplicity, we denote matrix \mathbf{P} as $\mathbf{P} = [P_1, \dots, P_j, \dots, P_{n+1}]$ and P_j is the j^{th} column vector of \mathbf{P} . That means,

$$P_j = [P_{1j}, P_{2j}, \dots, P_{ij}, \dots, P_{(n+1)j}]^T, \quad (18)$$

where P_{ij} is obtained from Theorem 1 in (13).

Because S_{n+1} is the absorbing state of the matrix \mathbf{P} , $[\pi^{(0)} \mathbf{P}^m]_{(n+1)}$ represents the probability that node w moves outside node u 's transmission zone within m time steps. Then the CDF of link lifetime can be obtained by:

$$\begin{aligned} Prob\{T_L \leq m\} &= Prob\{\rho_m > R_e \mid \rho_0 \leq R_e\} \\ &= [\pi^{(0)} \mathbf{P}^m]_{(n+1)} = \pi_{n+1}^{(m)}. \end{aligned} \quad (19)$$

The probability matrix \mathbf{P} is already determined by using Theorem 1. To find the stationary probability $\pi^{(0)}$, recall that the range of relative speed of two nodes is over $[0, 2(\bar{V} + \delta_V)]$. Hence, the maximum distance between a node-pair during each time step is $2(\bar{V} + \delta_V)$. This means the *maximum* number of states N of \mathbf{P} can be traveled during one time step is,

$$N = \left\lceil \frac{2(\bar{V} + \delta_V)}{\varepsilon} \right\rceil. \quad (20)$$

In Fig. 3, when node w moves across node u 's transmission zone, it may be at one of N possible states (from state S_n to S_{n-N+1}) at time t_0 . Here we assume that node w initially

lies in these N states with an equal probability as $1/N$ for determining the distribution $\pi^{(0)}$. Following (19) and (20), the PMF of link lifetime distribution is derived as:

$$\begin{aligned} \text{Prob}\{T_L = m\} &= \text{Prob}\{T_L \leq m\} - \text{Prob}\{T_L \leq m-1\} \\ &= [\pi^{(0)} \mathbf{P}^m]_{(n+1)} - [\pi^{(0)} \mathbf{P}^{m-1}]_{(n+1)}. \end{aligned} \quad (21)$$

In order to have a better understanding the above results, we simulate both the radio environments and smooth node mobility by ns-2. Specifically, the value of ETR can be configured by adjusting an appropriate value of the receiving threshold over the network interface. Because the current ns-2 physical module does not support multipath (Rayleigh) fading, we set up the receiving threshold according to the Shadowing propagation-model. Specifically, upon (4), the value of ETR is chosen from the set $\{94m, 149m, 200m, 239m, 286m, 342m\}$, which are obtained by considering typical urban micro-cells ($3 \leq \xi \leq 3.5$) superimposed with shadow fading ($\sigma_s \in [6, 9]dB$) [11]. TABLE I illustrates the relation between ETR with the corresponding radio environments.

TABLE I
THE ETR WITH RESPECT TO WIRELESS RADIO ENVIRONMENTS.

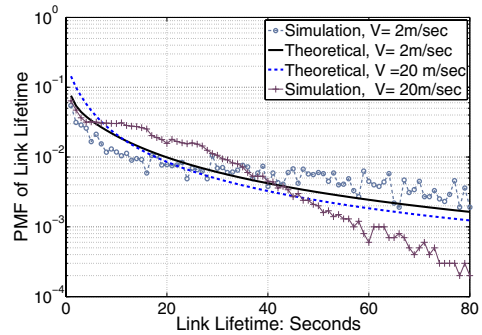
ETR (m)	94	149	200	239	286	342
ξ	3.5	3.5	3	3	3	3
σ_s (dB)	9	6	9	8	7	6

Here, we carried out multiple trials with 50 nodes with $R_e = 239$ m, uniformly distributed in an area of $1401m \times 1401m$ during a time period of 1000 seconds. The smooth user mobility [10] is set to zero pause time, 0.5 for temporal correlation parameter ζ , [20, 40] seconds for the moving phase, and [4, 6] seconds for acceleration and deceleration phases. Fig. 6(a) illustrates the link lifetime distribution with two mobility levels: low level ($\bar{V} = 2$ m/s) and high level ($\bar{V} = 20$ m/s). For clear demonstration, we show the results in the log-scale on Y-axis. According to Fig. 6(a), both theoretical and simulation results demonstrate that *link lifetime decreases exponentially with time regardless of the node speed and it decreases much quickly as the node speed is high*.

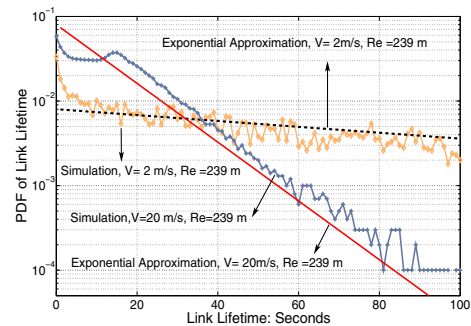
Interestingly, by taking a close look, we find that the PMF of link lifetime distribution can be approximated by an exponential distribution with parameter $\frac{\bar{V}}{R_e}$, which will be discussed in detail in Section IV-A, that is,

$$\begin{aligned} f_{T_L}(t) &\approx \frac{\bar{V}}{R_e} \cdot e^{(-\frac{\bar{V}}{R_e}t)}, \\ &= \frac{\bar{V}}{f(\xi, \sigma_s, \chi)} \cdot e^{(-\frac{\bar{V}}{f(\xi, \sigma_s, \chi)}t)}. \end{aligned} \quad (22)$$

The equation (22) in fact represents the PDF of link lifetime with continuous time t . It can be seen in Fig. 6(b) that this approximated exponential distribution characterized by the parameter $\frac{\bar{V}}{R_e}$, matches very well with the simulation results, especially for high speed. Recall, $R_e = f(\xi, \sigma_s, \chi)$, defined in (4), is a function of radio channel parameters: path loss (ξ), shadow fading (X_{σ_s}), and multi-path fading (χ^2). Hence, the parameter $\frac{\bar{V}}{R_e}$ in (22) indicates that the *link performance in mobile wireless network can be characterized by joint effects of radio channels and node mobility*.



(a) PMF of link lifetime.



(b) PDF approximation of link lifetime.

Fig. 6. Link lifetime distribution.

Remark 4: The link lifetime distribution can be effectively approximated by an exponential distribution with parameter $\frac{\bar{V}}{R_e}$, where \bar{V} is the average speed and R_e is the ETR of a mobile node. This result is in contrast with previous studies that there exists a peak in the distribution function which are mainly obtained from random mobility models [1]–[3].

IV. PROPERTIES OF LINK DYNAMICS

In this section, we discuss link properties such as average link lifetime, residual link lifetime, and link change rate. These link dynamics effectively reveal the changing frequency of network topology [12], [14], efficiency of routing operations [16], [17], and MANET application performance [2], [13].

A. Average Link Lifetime

From (21), the expected link lifetime \bar{T}_L is given by:

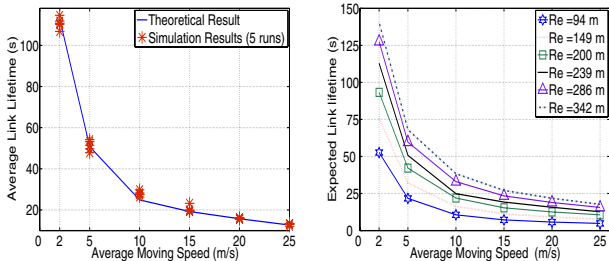
$$\bar{T}_L = \sum_{m=1}^{\infty} m([\pi^{(0)} \mathbf{P}^m]_{(n+1)} - [\pi^{(0)} \mathbf{P}^{m-1}]_{(n+1)}). \quad (23)$$

Given $R_e = 239m$, both theoretical and simulation results of \bar{T}_L with respect to average node speed \bar{V} are shown in Fig. 7(a), which match very well. Also, as the node speed increases, \bar{T}_L decreases dramatically when \bar{V} is within the range [2, 10] m/sec, and the downtrend of \bar{T}_L slows down when $\bar{V} > 10$ m/sec. More interestingly, we find that the \bar{T}_L can be estimated by the empirical equation $\hat{T}_L = R_e/\bar{V}$. Table II illustrates the results of both theoretical \bar{T}_L from (23) and estimated \hat{T}_L with respect to node mobility. The physical meaning of the equation

$\hat{T}_L = R_e/\bar{V}$ is the time a node takes to move across the radius of its neighbor's transmission zone at its average speed \bar{V} . This result could be used as an engineering approximation of link lifetime in ad hoc networks, especially for low mobility to medium mobility with speed less than 35 km/hour.

TABLE II
COMPARISON: \bar{T}_L AND ESTIMATED \hat{T}_L , FOR $R_e = 239$ M.

$V(m/s)$	2	5	10	15	20	25
$\bar{T}_L(s)$	112.94	50.75	24.89	19.23	15.72	12.68
$\hat{T}_L(s)$	119.5	47.8	23.9	15.9	12.0	9.6



(a) Average link lifetime. (b) ETR impacts.
Fig. 7. Average link lifetime.

Based on the theoretical results on (23), we further investigate the ETR effect on average link lifetime \bar{T}_L with different node mobility. The results are shown in Fig. 7(b). We find that the larger R_e is, the longer the \bar{T}_L is obtained, which is consistent with our expectation. However, it can be observed that the ETR has much more significant impact on \bar{T}_L for nodes with low mobility than those with high mobility.

Remark 5: For an ad hoc network with lower node mobility, or even without node mobility such as static sensor networks, \bar{T}_L is predominated by ETR, i.e., radio channel characteristics. For a network with faster mobile nodes such as vehicular ad hoc networks, \bar{T}_L is dominated by node speed.

B. Residual Link Lifetime

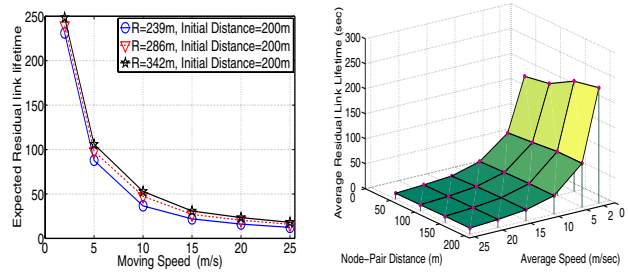
Residual link lifetime T_R is the remaining link duration after the link is established. It can be interpreted by link availability $L(\rho_m^{(i)}, m')$, which is a probability that a link will be continuously available at least m' steps given that the link exists m time steps with node-pair distance ρ_m in state S_i .

$$L(\rho_m^{(i)}, m') = \frac{Prob\{T_L \geq m' + m\}}{Prob\{T_L > m \mid \rho_m \in S_i\}}. \quad (24)$$

Therefore, upon the definition of link availability $L(\rho_m^{(i)}, m')$ in (24), the corresponding PMF of residual link lifetime T_R is represented as

$$\begin{aligned} Prob\{T_R = m'\} &= L(\rho_m^{(i)}, m' - 1) - L(\rho_m^{(i)}, m') \\ &= [\pi_{i,1}^{(m)} \mathbf{P}^{m'}]_{(n+1)} - [\pi_{i,1}^{(m)} \mathbf{P}^{m'-1}]_{(n+1)}, \end{aligned} \quad (25)$$

where $\pi_{i,1}^{(m)}$ is a vector in which the i -th element is equal to 1, while other elements are equal to 0. This means, after m -th time step, the probability $Prob\{\rho_m \in S_i\} = 1$.



(a) ETR vs. speed. (b) Relative distance vs. speed.

Fig. 8. Effects on average residual link lifetime.

Due to the page limit, we only shows our main results of residual link lifetime in Fig. 8. In particular, by comparing Fig. 8(a) with Fig. 7(b), we found that the impacts of ETR and node mobility on the \bar{T}_R is very similar to those on the \bar{T}_L . Furthermore, given $R_e = 239$ m, Fig. 8(b) illustrates the influence of initial node-pair distance on \bar{T}_R with respect to different node speeds. It is interesting to see that for a specific average speed, the average residual link lifetime, does not vary significantly with node-pair distance, especially for high speed mobile nodes.

Remark 6: Similar to the link lifetime, the impacting factors on residual link lifetime are in the decreasing order of average node speed, ETR, and node-pair distance.

C. Link Change Rate

Radio links among nodes in ad hoc networks have an immediate effect on network topology. More specifically, average link change rate η_L is the the expected number of link changes per second observed by a single node, which is sum of *link breakage rate* and *link arrival rate*. Based on the result in [3], we know that $\eta_L = 2\lambda$, where λ is the link arrival rate.

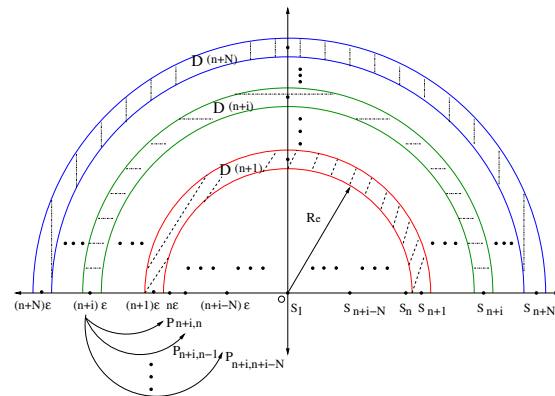


Fig. 9. Derivation of expected link arrival rate λ .

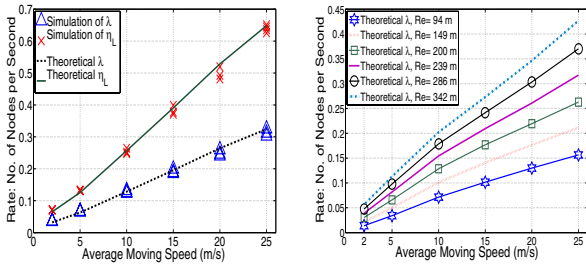
Upon Fig. 3, link arrival rate λ is equivalent to the expected number of new nodes entering node u 's transmission zone at every time step. Thus, we extend the total number of states of matrix \mathbf{P} from $n+1$ to $n+N$, where N is obtained in (20). The extended states are shown in Fig. 9. Hence, a node could enter node u 's transmission zone at the next time step, only if it is currently lying in one of the states $\{S_{n+1}, S_{n+2}, \dots, S_{n+N}\}$. Let $P_L(n+i)$ denote the probability that a node in state S_{n+i}

will move into node u 's transmission zone during the next time step movement. Then, $P_L(n+i)$ is given by:

$$P_L(n+i) = \sum_{j=n+i-N}^n P_{n+i,j}, \quad 1 \leq i \leq N, \quad (26)$$

where $P_{n+i,j}$ can be obtained from the approximation equation (13). Furthermore, for S_{n+i} , we denote the region \mathbf{D}_{n+i} as the set of all positions that are in distance of $[(n+i-1)\varepsilon, (n+i)\varepsilon]$ away from the reference node u . This set actually covers the region of a circular ring with the outer radius $(n+i)\varepsilon$ and the inner radius $(n+i-1)\varepsilon$, respectively. Hence, we have the area of \mathbf{D}_{n+i} , $S(\mathbf{D}_{n+i}) = \pi\varepsilon^2[(n+i)^2 - (n+i-1)^2] = \pi\varepsilon^2(2i+2n-1)$. Using the same assumption in [3], [14] that node density σ follows the uniform distribution, then $\sigma \cdot S(\mathbf{D}_{n+i})$ is the average number of nodes lying within \mathbf{D}_{n+i} . Therefore, the total number of possible nodes moving into node u 's transmission zone at the next time step is the summation of the number of nodes currently lying at all possible regions \mathbf{D}_{n+i} , $1 \leq i \leq N$. Then, we have

$$\begin{aligned} \lambda &= \sum_{i=1}^N P_L(n+i) \cdot \sigma \cdot S(\mathbf{D}_{n+i}) \\ &= \sigma\pi\varepsilon^2 \sum_{i=1}^N \sum_{j=n+i-N}^n P_{n+i,j} \cdot (2i+2n-1). \end{aligned} \quad (27)$$



(a) Node mobility.

(b) ETR impacts.

Fig. 10. Factors impacts on λ and η_L .

In Fig. 10(a), we compare the analytical and simulation results of average link change rate η_L , where $R_e = 239m$. As can be observed, the analytical results closely match the the simulation results. From Fig. 10(b), it is clear that ETR R_e has much more significant impact on λ for nodes with higher mobility than that with lower mobility.

V. IMPLICATIONS ON NETWORK TOPOLOGY AND PERFORMANCE

By far, we mainly investigated the significance of radio channels and node mobility on the link dynamics. Next, by applying these knowledge, we will demonstrate the implication of link dynamics on path lifetime, network connectivity, and routing performance of ad hoc networks, which is our another objective in this study.

A. k -hop Path Lifetime

To study the path properties, we assume that the stochastic properties of different links incident to a path are identical and links fail independently. In reality, there may exist correlation between two adjacent links which share the same node, so that

the adjacent links could break at the same time. Compared to the independent link failure cases along paths in ad hoc networks, this correlated link failure scenario happens much less. This assumption has been shown to apply well for deriving the path properties [2], [3], [7]. Since the path lifetime is determined by the minimum link lifetime en route, as shown in (22), we can easily conclude that *the PDF of path lifetime also follows exponential distribution with the parameter λ_P* [20], which greatly relaxes the assumption of $k \rightarrow \infty$ for its distribution converging to exponential distribution [9]. In particular, the parameter $\lambda_P = \sum_{1 \leq l \leq k} \frac{\bar{V}_l}{R_{el}}$, where R_{el} and \bar{V}_l are the associated ETR and average node speed for the l^{th} link along the k -hop path.

Remark 7: The probability distribution function of path lifetime follows exponential distribution for any k -hop path, with parameter of λ_P , which is the summation of exponential parameters of each link along the path.

B. Network Connectivity

Here, we apply the knowledge of average link lifetime \bar{T}_L and average link change rate η_L to investigate their relationship with the average node degree for estimating the network connectivity. Let $\kappa(G(t))$ and $E\{d_{G(t)}\}$ be the connectivity and average degree of a network $G(t)$, respectively. According to Graph Theory [21], if $\kappa(G(t)) = \kappa$, then the network $G(t)$ is κ -connected at time t , and $\kappa(G(t)) \leq E\{d_{G(t)}\}$. Thus, $E\{d_{G(t)}\}$ is the upper bound of the connectivity of $G(t)$. Let each node in $G(t)$ be associated with a queuing system. For instance, in node u 's queuing system, an arrival event means the event that a node moves inside node u 's transmission zone, and a departure event represents a current neighbor node moves outside node u 's transmission zone. Then, according to the Little's law of a queuing system: the average number of customers in the system, i.e., $E\{d_{G(t)}\}$, is equal to the average arrival rate, i.e., λ , of customer to the system multiplied by the average system time, i.e., \bar{T}_L , per customer. Therefore, we can apply \bar{T}_{link} and η_L to estimate the upper bound connectivity of a network,

$$\kappa(G(t)) \leq E\{d_{G(t)}\} = \lambda \cdot \bar{T}_L = \frac{1}{2}\eta_L \cdot \bar{T}_L, \quad (28)$$

where \bar{T}_L and η_L are derived from (23) and (27), respectively.

C. Routing Performance

Furthermore, we investigate the impacts of link dynamics on routing performance by taking AODV as a case study in ns-2. The network traffic is composed of 20 constant bit rate (CBR) sources and 30 connections among total 50 nodes. And each source sends 1 packet/sec with the packet size 64 bytes. The value of ETR is chosen from the set $\{94m, 149m, 200m, 239m, 286m, 342m\}$, which are obtained by considering radio channels shown in TABLE I. From Fig.11(a) and 11(b), it can be seen that the performance of average end-to-end packet delay and throughput increases substantially as the rise of ETR R_e . However, in Fig.11(b) when $R_e \leq 239m$, the routing performance is not acceptable

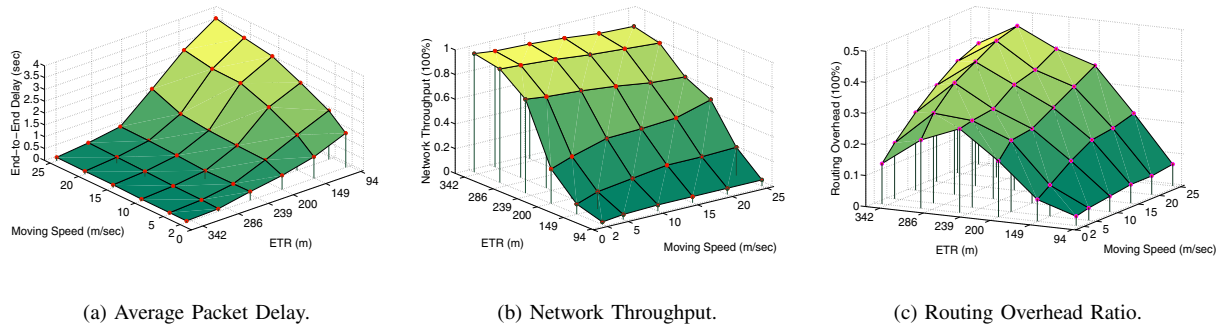


Fig. 11. Effective transmission range and node mobility impacts on AODV routing performance.

for practical applications, because of network dis-connectivity due to lack of neighboring nodes. Interestingly, from Fig.11(c), we find that the routing overhead increases when R_e rises from [94, 286]m, and it start to reduce regardless of node speed when $R_e > 286$ m. This is because the increasing number of neighboring nodes is large enough to almost always form a connected network, while dramatically reducing the number of path updates. Thus, we find that routing protocols should only be evaluated and studied under certain range of node density, where the statistics of link properties can be well applied to improve the routing efficiency as well as the network performance. Upon the illustration of simulation results and Table III, we have the following observation regarding the effect of node density on routing performance.

Remark 8: The routing performance varies sensitively and can be effectively improved by applying the knowledge of link dynamics when the number of nodes per transmission zone, σ_R , changes from 5 to 10.

TABLE III
NODE DENSITY σ_R VS. AVERAGE NODE DEGREE $E\{d_G(t)\}$.

R_e	94	149	200	239	286	342
$\sigma_R = No./\pi R_e^2$	0.7	1.8	3.2	4.6	6.5	9.3
$E\{d_G(t)\}$	0.52	1.62	2.82	4.35	6.05	7.9

VI. CONCLUSIONS

In this paper, we studied the joint effects of radio channels and node mobility on link lifetime and its properties. Our results include: i) radio channel characteristics predominate the link performance for slower mobile nodes, while node mobility dominates the link performance for faster mobile nodes; ii) link lifetime can be effectively approximated by exponential distribution with parameter $\frac{\bar{V}}{R_e}$; iii) the impacting factors on both link and residual link lifetime are in the decreasing order of average node speed \bar{V} , ETR, and node-pair distance; and iv) k -hop path lifetime can also be characterized by exponential distribution for any arbitrary hop-count k . As a fundamental study, our analytical results and simulation findings on link dynamics can be readily applied to system design such as topology control and routing optimization.

REFERENCES

[1] M. Gerharz, C. Waal, M. Frank, and P. Martini, "Link stability in mobile wireless ad hoc networks," in *Proc. of IEEE Local Computer Networks LCN*, 2002.

[2] N. Sadagopan, F. Bai, B. Krishnamachari, and A. Helmy, "Paths: Analysis of path duration statistics and their impact on reactive manet routing protocols," in *Proc. of ACM MobiHoc*, June 2003.

[3] P. Samar and S. B. Wicker, "On the behavior of communication links of node in a multi-hop mobile environment," in *Proc. of ACM MobiHoc*, May 2004.

[4] X. Wu, H. R. Sadjadpour, and J. J. Garcia-Luna-Aceves, "An analytical framework for the characterization of link dynamics in manets," in *Proc. IEEE MILCOM*, October 2006.

[5] S. Xu, K. Blackmore, and H. Jones, "Assessment for manets requiring persistent links," in *Proc. of International Workshop on WitMeMo*, 2005.

[6] X. Hong, T. J. Kwon, M. Gerla, D. L. Gu, and G. Pei, "A mobility framework for ad hoc wireless networks," in *Proc. of International Conference on Mobile Data Management (MDM)*, 2001.

[7] A. B. McDonald and T. F. Znati, "A mobility-based framework for adaptive clustering in wireless ad hoc networks," *IEEE Journal on Selected Areas in Communications*, vol. 17, no. 8, pp. 1466–1487, August 1999.

[8] S. Jiang, "An enhanced prediction-based link availability estimation for manets," *IEEE Transactions on Communications*, vol. 52, no. 2, pp. 183–186, February 2004.

[9] R. J. La and Y. Han, "Distribution of path durations in mobile ad-hoc networks and path selection," in *Proc. of Infocom*, 2006.

[10] M. Zhao and W. Wang, "A novel semi-markov smooth mobility model for mobile ad hoc networks," in *Proc. of IEEE GLOBECOM*, 2006, (best student paper award).

[11] M. Schwartz, *Mobile Wireless Communications*, 1st ed. CAMBRIDGE, 2005.

[12] D. Miorandi and E. Altman, "Coverage and Connectivity of Ad-Hoc Networks in Presence of Channel Randomness," in *Proc. of IEEE INFOCOM'05*, March 2005.

[13] C. E. Koksal, K. Jamieson, E. Telatar, and P. Thiran, "Impacts of Channel Variability on Link-Level Throughput in Wireless Networks," in *Proc. of SIGMetrics Performance*, 2006.

[14] C. Bettstetter and C. Hartmann, "Connectivity of wireless multihop networks in a shadow fading environment," *ACM/Kluwer Wireless Networks*, vol. 11, no. 5, pp. 571–579, September 2005.

[15] K.-J. Yang and Y.-R. Tsai, "Link stability prediction for mobile ad hoc networks in shadowed environments," in *Proc. of IEEE GLOBECOM*, 2006.

[16] F. Bai, N. Sadagopan, B. Krishnamachari, and A. Helmy, "Important: A framework to systematically analyze the impact of mobility on performance of routing protocols for ad hoc networks," in *Proc. of IEEE INFOCOM*, 2003.

[17] Z. Cheng and W. Heinzelman, "Exploring Long Lifetime Routing (LLR) in ad hoc networks," in *Proc. of ACM International Symposium on MSWiM*, 2004.

[18] L. Booth, J. Bruck, M. Cook, and M. Franceschetti, "Ad hoc wireless networks with noisy links," in *Proc. of ISIT*, 2003.

[19] "Accutech: Factors affecting transmission distance." [Online]. Available: <http://www.accutechinstruments.com/downloads/technical-articles/tech-note-215-transmission-distance.pdf>

[20] A. Papoulis, *Probability, Random Variables, and Stochastic Process*. McGraw-Hill, 1991.

[21] D. B. West, *Introduction to Graph Theory*, 2nd ed. Prentice-Hall, 2000.